

# Detection of Bias in GPS satellites' Measurements for Enhanced Measurement Integrity

Mamoun F. Abdel-Hafez

**Abstract**—In this paper, the detection of a fault in the Global Positioning System (GPS) measurement is addressed. The class of faults considered is a bias in the GPS pseudorange measurements. This bias is modeled as an unknown constant. The fault could be the result of a receiver fault or signal fault such as multipath error. A bias bank is constructed based on set of possible fault hypotheses. Initially, there is equal probability of occurrence for any of the biases in the bank. Subsequently, as the measurements are processed, the probability of occurrence for each of the biases is sequentially updated. The fault with a probability approaching unity will be declared as the current fault in the GPS measurement. The residual formed from the GPS and Inertial Measurement Unit (IMU) measurements is used to update the probability of each fault. Results will be presented to show the performance of the presented algorithm.

**Keywords**—Estimation and filtering; Statistical data analysis; Fault detection and identification.

## I. INTRODUCTION

With the increase in the number of integrated sensors used in current engineering applications, sensor fusion research is ongoing to increase the accuracy of obtaining high-accuracy estimates from sensors' measurements. Systems that are expected to work autonomously need to be designed carefully to ensure accurate operation under changing operational environments. Also, sensors might degrade in performance over time. Sensors' quality becomes an important issue for such systems. The designer has the option of selecting sophisticated and accurate sensors on the expense of cost. Alternatively, he can adapt less expensive sensors and design his fusion algorithm to account for the less-accurate measurements [1].

One of the widely used sensors for autonomous applications is the GPS and IMU sensors, [2], [3], [4]. In this paper, the problem of detecting and identifying bias in the GPS pseudorange measurements is addressed. A probabilistic approach is used to identify bias error on the GPS pseudorange measurements. A number of hypotheses of possible bias errors, including a zero bias hypothesis, in the measurements are first constructed. At the beginning, the GPS measurements can have any of these bias hypotheses. As measurements are sampled, the probability of each hypothesis is updated and the hypothesis for which the probability approach unity is declared the true bias in the GPS measurements. The probabilistic fault detection filter makes use of the GPS/IMU measurements in constructing the residual used to update the probability.

The problem of integrity monitoring of dynamic systems is being investigated by many researchers. In references [5], [6],

researchers try to identify possible degradation in the dynamics and measurements noise statistics. In reference [7], the authors approach the detection of interference/jamming and spoofing in a DGPS-aided inertial system. Interference and jamming are modeled as increase in GPS noise covariance. Spoofing is modeled as a bias in the GPS measurement. A multiple model adaptive estimator (MMAE) is used to detect the covariance of the GPS measurements from a set of assumed failure hypotheses. On the other hand, a moving-bank pseudo-residual MMAE is used to detect and identify spoofing.

In this study, a baseband ultra-tightly coupled GPS/IMU filter structure is implemented to check the performance of the proposed algorithm in detecting and estimating different GPS pseudorange measurements bias levels, Figure 1. In the figure,  $h_{\Delta}()$  is the discriminator function acting on the timing error between the received code signal and its locally generated replica,  $\Delta$  is the time spacing between early and late paths in number of chips,  $T_c$  is the chip period,  $t_d$  is the true time,  $\hat{t}_d$  is the estimated time,  $k$  is the filter gain,  $p$  is the signal amplitude, and  $n'$  is the additive white Gaussian noise. The output of the navigation filter is used to control a voltage controlled oscillator (VCO) or a numerically controlled oscillator (NCO), which in turn controls the local Pseudo Noise (PN) code generator. In the ultra-tight filter structure, the IMU measures the receiver motion and helps isolate the GPS measurement noise from the true measurement. To estimate the state of the receiver accurately, there is a need to know the bias in the GPS pseudorange measurements. This bias might be due to many factors such as receiver fault, GPS signal fault, and/or signal multipath. This motivated the need for estimation methods applied to GPS measurements bias detection and identification.

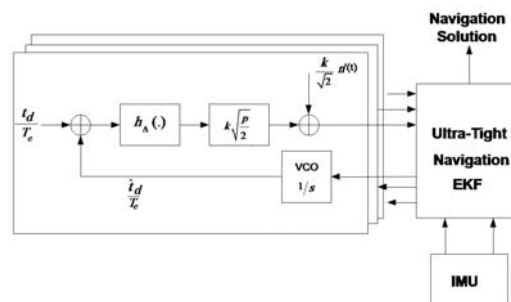


Fig. 1. Ultra-Tightly Coupled GPS/IMU fusion Structure

The GPS/IMU measurements are described next.

Mamoun F. Abdel-Hafez is with the Department of Mechanical Engineering, American University of Sharjah, United Arab Emirates, e-mail: mabdelhafez@aus.edu

## II. GPS/IMU MEASUREMENTS

The GPS measurements include the C/A code measurements, the carrier phase measurements, and the range rate measurements. These measurements can be acquired on two wave frequencies  $L_1$  and  $L_2$ . The proposed algorithm can be used to estimate the measurement noise statistics of any of these measurements. Nevertheless, in this study, the C/A pseudorange measurements are used and their measurement noise statistics are estimated.

The IMU measures the angular velocity,  $\omega_{EB}^B$ , and the linear acceleration,  $f^B$ , of the platform in three perpendicular directions. The IMU is used to construct the dynamics equation that defines the time propagation of the platform state. By measuring the dynamics of the vehicle, the IMU assist the code-tracking loop in keeping track of the GPS code signal.

The state of the vehicle at any time is defined in terms of its position, velocity, and attitude. The position,  $P^E$ , and velocity,  $V^E$ , are represented in terms of the Earth Centered, Earth Fixed (ECEF) coordinate system while the attitude,  $Q_B^E$  is represented in quaternion format and describes the body frame orientation relative to the ECEF frame. The dynamics of this state is obtained by differentiating the state variables and is represented as:

$$\dot{P}^E = V^E \quad (1)$$

$$\dot{V}^E = C_B^E f^B - 2\omega_{IE}^E \times V^E + G^E \quad (2)$$

$$\dot{Q}_B^E = \frac{1}{2} \Omega_{EB}^B Q_B^E \quad (3)$$

where,  $C_B^E$  is the cosine rotation matrix from the body frame to the ECEF frame,  $\omega_{IE}^E$  is the angular velocity of earth relative to the inertial frame represented in the ECEF frame, and  $G^E$  is the gravity vector in the ECEF frame.  $f^B$  is the specific force of the vehicle represented in the body frame and  $\omega_{EB}^B$  is the angular velocity of the body frame relative to the ECEF frame represented in the body frame. These two vectors define the evolution of the state of the vehicle.  $\Omega_{EB}^B$  is defined as:

$$\Omega_{EB}^B = \begin{bmatrix} 0 & -\omega_x & -\omega_y & -\omega_z \\ \omega_x & 0 & \omega_z & -\omega_y \\ \omega_y & -\omega_z & 0 & \omega_x \\ \omega_z & \omega_y & -\omega_x & 0 \end{bmatrix}$$

where:  $\omega_{EB}^B = [\omega_x \ \omega_y \ \omega_z]$

Equations 1 to 3 are linearized to obtain the dynamic equation of the vehicle [8], [9], [10].

## III. SEQUENTIAL RESIDUAL PROCESSING AND FAULT DETECTION

In this section, a sequential bias detection technique is proposed for identifying a possible GPS pseudorange measurements bias fault. The formulation of the method for the time-varying GPS/IMU system is described. Given that the GPS/IMU system is represented in the time-varying system model [8], [9], [10]:

$$\mathbf{x}_{k+1} = \phi_k \mathbf{x}_k + \mathbf{B}_k \mathbf{w}_k \quad (4)$$

$$\mathbf{z}_k = \mathbf{H}_k \mathbf{x}_k + \mathbf{v}_k \quad (5)$$

The linear state estimator is given as:

$$\begin{aligned} \bar{\mathbf{x}}_{k+1} &= \phi_k \hat{\mathbf{x}}_k \\ \hat{\mathbf{x}}_k &= \bar{\mathbf{x}}_k + \mathbf{K}_k [\mathbf{z}_k - \mathbf{h}(\bar{\mathbf{x}}_k)] \end{aligned}$$

where  $\bar{\mathbf{x}}_{k+1}$  denotes the estimate of the error state given all the measurements up to time  $k$ ,  $\hat{\mathbf{x}}_k$  is the posteriori error state estimate given all the measurements up to time  $k$ ,  $\mathbf{K}_k$  is the filter gain,  $\mathbf{h}(\bar{\mathbf{x}}_k) = \|\bar{P}^E - P^K\|$ . Defining the estimation error as:  $\epsilon_k = \mathbf{x}_k - \bar{\mathbf{x}}_k$ , the measurement residual is defined as:

$$\mathbf{r}_k = \mathbf{z}_k - \mathbf{H}_k \bar{\mathbf{x}}_k \quad (6)$$

It is assumed that a bias in satellite pseudorange measurement  $j$  is written as  $\mu^j$ . It is assumed that a bias will occur in one satellite at a time. Furthermore, it is assumed that this bias will be detected and corrected before the occurrence of other faults in the satellite's or other satellites' measurements. Therefore, the measurement vector  $\mathbf{z}_k$  is written as:

$$\mathbf{z}_k = \mathbf{H}_k \mathbf{x}_k + \mathbf{v}_k + \boldsymbol{\mu} \quad (7)$$

where the measurement error vector  $\boldsymbol{\mu}$  is defined as:

$$\boldsymbol{\mu} = \begin{bmatrix} 0 \\ 0 \\ \mu^j \\ 0 \\ \vdots \\ 0 \end{bmatrix} \quad (8)$$

The residual process can be written as:

$$\mathbf{r}_k = \mathbf{H}_k \epsilon_k + \mathbf{v}_k + \boldsymbol{\mu} \quad (9)$$

A projector  $\mathbf{N}$  is defined as:

$$\mathbf{N} = \mathbf{I} - \mathbf{H}_k (\mathbf{H}_k^T \mathbf{H}_k)^{-1} \mathbf{H}_k^T \quad (10)$$

The projector is in the null space of  $\mathbf{H}_k$  and is multiplied by  $\mathbf{r}_k$  to get a sequential residual that is only a function of the measurement error and the possible bias fault. It can be seen that:

$$\mathbf{N} \mathbf{r}_k = \mathbf{N} (\mathbf{v}_k + \boldsymbol{\mu}) \quad (11)$$

The singular value decomposition of the projector  $\mathbf{N}$  is used to characterize the statistics of the modified residual process:

$$\mathbf{N} = [\mathbf{U}_1 \ \mathbf{U}_2] \begin{bmatrix} \mathbf{I} & \mathbf{0} \\ \mathbf{0} & \mathbf{0} \end{bmatrix} \begin{bmatrix} \mathbf{V}_1 \\ \mathbf{V}_2 \end{bmatrix} \quad (12)$$

where  $\mathbf{U}_1$  is full column rank with  $\mathbf{U}_1^T \mathbf{U}_1 = \mathbf{I}$  and  $\mathbf{V}_1$  is full row rank with  $\mathbf{V}_1 \mathbf{V}_1^T = \mathbf{I}$ . Therefore,

$$\begin{aligned} \mathbf{N} \mathbf{r}_k &= [\mathbf{U}_1 \ \mathbf{U}_2] \begin{bmatrix} \mathbf{I} & \mathbf{0} \\ \mathbf{0} & \mathbf{0} \end{bmatrix} \begin{bmatrix} \mathbf{V}_1 \\ \mathbf{V}_2 \end{bmatrix} (\mathbf{v}_k + \boldsymbol{\mu}) \\ &= [\mathbf{U}_1 \ \mathbf{0}] \begin{bmatrix} \mathbf{V}_1 \\ \mathbf{V}_2 \end{bmatrix} (\mathbf{v}_k + \boldsymbol{\mu}) \end{aligned} \quad (13)$$

This can be rewritten as:

$$\mathbf{U}_1 \mathbf{V}_1 \mathbf{r}_k = \mathbf{U}_1 \mathbf{V}_1 (\mathbf{v}_k + \boldsymbol{\mu}) \quad (14)$$

Premultiplying equation 14 by  $U_1^T$  we get:

$$\tilde{\mathbf{r}}_k = \mathbf{V}_1 \mathbf{r}_k = \mathbf{V}_1 (\mathbf{v}_k + \boldsymbol{\mu}) \quad (15)$$

For each satellite in view, a number of bias hypotheses will be selected. One of these hypotheses is the null hypothesis where the satellite have zero bias. Therefore, the fault hypothesis  $H_{i,j}$  is the hypothesis that satellite  $i$  have a bias of magnitude  $\mu^j$ . Based on this, the mean and covariance of tilder given a certain hypothesis can be defined as:

$$\bar{\mathbf{r}} = \mathbf{E}[\tilde{\mathbf{r}}|H_{i,j}] = \mu^j \mathbf{V}_1^i \quad (16)$$

$$\boldsymbol{\Gamma}_r = \mathbf{E}[\tilde{\mathbf{r}}\tilde{\mathbf{r}}^T|H_{i,j}] = \sigma_v^2 \mathbf{V}_1 \mathbf{V}_1^T \quad (17)$$

where  $\mathbf{V}_1^i$  is the  $i_{th}$  column of  $\mathbf{V}_1$ . Since  $\tilde{\mathbf{r}}$  is Gaussian, its probability density function given a certain bias hypothesis is given by:

$$\mathbf{f}_{\tilde{\mathbf{r}}|H_{i,j}}(\tilde{\mathbf{r}}|H_{i,j}) = \frac{1}{(2\pi)^{n/2} |\boldsymbol{\Gamma}_r|^{1/2}} \exp^{-\frac{1}{2}(\tilde{\mathbf{r}}-\bar{\mathbf{r}})^T \boldsymbol{\Gamma}_r^{-1} (\tilde{\mathbf{r}}-\bar{\mathbf{r}})} \quad (18)$$

The probability that the  $l_{th}$  hypothesis where the  $i_{th}$  satellite has a bias of magnitude  $\mu^j$  can be shown to be:

$$\mathbf{F}_{k+1,l} = \frac{\mathbf{F}_{k,l} \mathbf{f}_{\tilde{\mathbf{r}}|H_1}(\tilde{\mathbf{r}}|H_1)}{\sum_{l=0}^M \mathbf{F}_{k,l} \mathbf{f}_{\tilde{\mathbf{r}}|H_1}(\tilde{\mathbf{r}}|H_1)} \quad (19)$$

where,  $\mathbf{F}_{k+1,l}$  is the probability that the  $l_{th}$  hypothesis occurs given all the measurements up to time  $k+1$ ,  $M$  is the total number of hypotheses. If the number of satellites in view is  $m$  and the number of hypothesis per satellite is  $p$ , then the number of hypotheses  $M$  can be shown to be:

$$M = m * (p - 1) + 1$$

This algorithm is used to estimate bias in the GPS pseudorange measurements. The GPS/IMU EKF is given enough time to allow the state and the covariance matrix to converge; in this application this time is 10 seconds. A bank of possible bias magnitudes in satellite measurements is then hypothesized. These hypotheses are initialized with equal probability. Subsequently, the proposed algorithm updates the probability of each hypothesis in the bank of residual, see equation 19. The hypothesis with probability that converge to one is declared the correct bias in the GPS pseudorange measurement. Once the GPS pseudorange bias is estimated, it is then corrected in the GPS/IMU EKF allowing for an improved-accuracy state estimate. The algorithm should be repeated periodically to account for any change in the GPS receiver environment or the instruments performance.

#### IV. SIMULATION RESULTS

A simulation environment was built to test the algorithms presented in this paper, see Figure 1. The trajectory of the vehicle was set to begin at a certain position, then input linear acceleration and angular velocity were integrated to obtain the true vehicle position, velocity, and attitude. Based on the position of the vehicle, GPS satellites' C/A code measurements were simulated. These measurements were used as input to our noise-estimation algorithm. The input linear acceleration is

shown in Figure 2. As seen in the figure, the vehicle was given high acceleration to simulate a harsh environment. The vehicle was simulated to have small angular velocity. This trajectory profile guarantees an observable GPS/IMU system, references [9], [11]. The ultra-tightly coupled GPS/IMU filter structure should be able to operate in this high-dynamics environment since the dynamics of the system are fed back to the code-tracking loop. By estimating bias in the GPS pseudorange measurement, the integrity and accuracy of the GPS/IMU system is considerably enhanced.

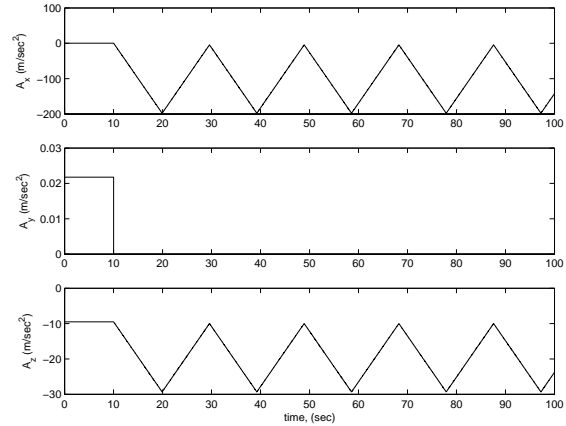


Fig. 2. Vehicle Acceleration Profile

The algorithm was tested for a number of GPS measurement bias magnitudes. The bias was assumed to affect one satellite at a time. Along with the null hypothesis of no bias error existing on the GPS measurement, four other hypotheses were assumed. The four hypotheses were distributed around the null hypothesis. In practice, enough hypotheses should be assumed to cover possible bias error levels. If the bias affecting the GPS measurement is close to one of the hypotheses, then the probability of that hypothesis will approach unity. Then that hypothesis is declared the true hypothesis. Figures 3 to 10 present the performance of the proposed algorithm.

Figures 3 to 5 show the probability of three hypotheses out of the hypothesis set. In these figures, the GPS pseudorange measurement noise covariance matrix is set to be a unity covariance matrix. The correct bias level is varied and the algorithm is tested to show if it can detect this bias level.

In figure 3 the correct bias level is 10 m on the second satellite in the measurement set. This bias level is among the hypothesis set that is initially constructed in the filter. The probability for this hypothesis is presented in the third plot in figure 3. It can be seen that the probability of the hypothesis quickly approaches unity and the algorithm therefore successfully detects this bias.

In figure 4, the correct bias level is 7 m on the second satellite in the measurement set. There is no hypothesis associated with this fault level. This bias exist between a hypothesis of 5m and another of 10m. The probability associated with these hypotheses is plot 2 and 3 of figure 4. It can be seen that the algorithm divides the probability of one between these two hypotheses where the algorithm gives zero probability to

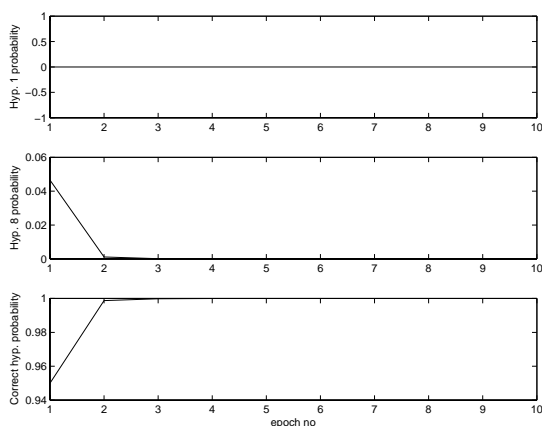


Fig. 3. Hyp. Probability, 10m-bias, Meas. Cov. = 1

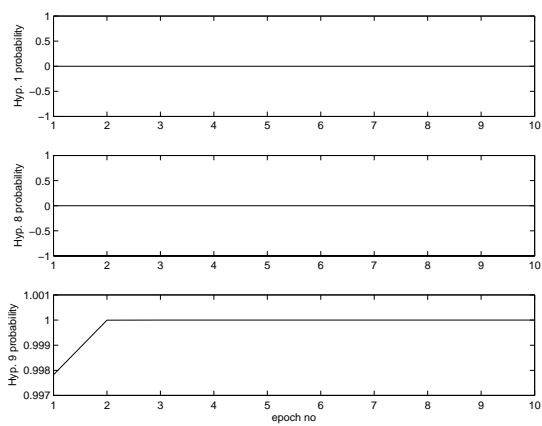


Fig. 5. Hyp. Probability, 20m-bias, Meas. Cov. = 1

other hypotheses in the hypothesis set as shown in the first plot of figure 4.

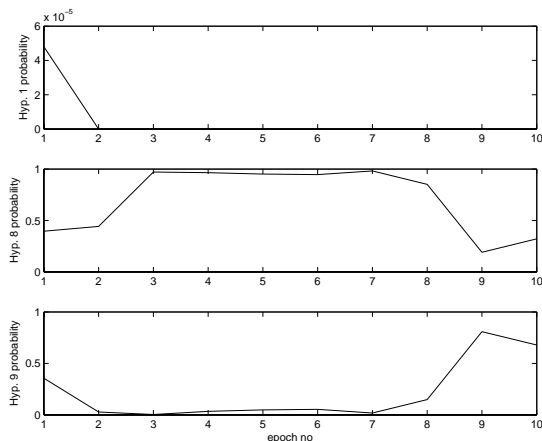


Fig. 4. Hyp. Probability, 7m-bias, Meas. Cov. = 1

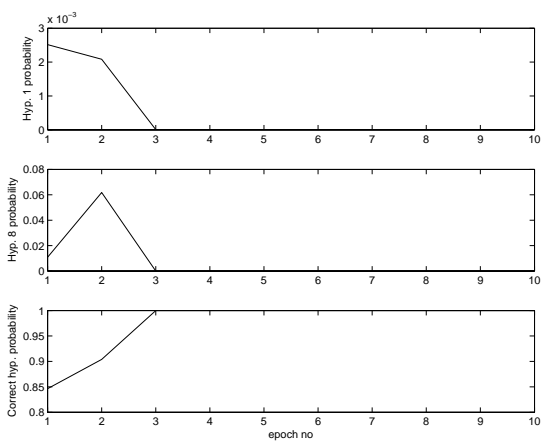


Fig. 6. Hyp. Probability, 10m-bias, Meas. Cov. = 2.1

In figure 5, the correct bias level is 20m added to the second satellite in the measurement set. This bias level is not one of the assumed bias hypotheses for this satellite. The closest hypothesis is 10m. The probability associated with this hypothesis is shown in plot 3 of figure 5. It can be seen that the algorithm assigns a probability of one to this hypothesis while it gives a probability of zero to the other hypotheses.

In figures 6 to 8, the algorithm was tested when the GPS measurement noise covariance matrix is increased to 2.1 unity matrix. Again, the correct bias level is varied and the performance of the proposed algorithm in detecting the correct measurement bias is shown.

In figure 6, the correct bias level is 10m on the third satellite. This bias level is one of the assumed bias levels in the hypothesis set. The probability for this bias is shown in the third plot in figure 6. It can be seen that the algorithm still detects the correct bias level but in a slower speed than when the GPS measurement noise standard deviation is smaller as seen in figure 3.

In figure 7, the correct bias level is 7m on the third satellite.

This bias level is not one of the hypothesized bias levels but falls between a hypothesis of 5m and another of 10m. It can be seen that the algorithm distributes the sure probability of 1 between these two hypotheses which are shown in plots 2 and 3 of figure 7.

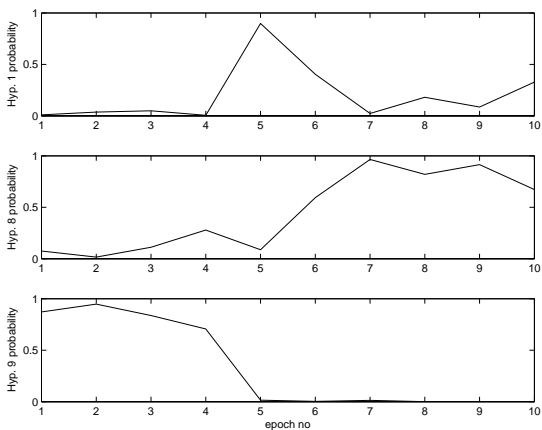


Fig. 7. Hyp. Probability, 7m-bias, Meas. Cov. = 2.1

In figure 8 the correct measurement bias is 20 m on the third satellite. This bias level is not one of the hypothesized measurement bias magnitudes. It can be seen that the algorithm assigns a probability of 1 to the closest hypotheses which is a hypothesis of 10 m bias.

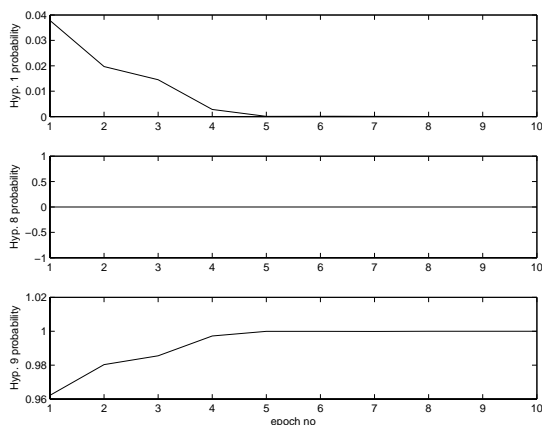


Fig. 8. Hyp. Probability, 20m-bias, Meas. Cov. = 2.1

Finally, the algorithm is tested when the GPS measurement noise covariance matrix is set to 12.5 diagonal matrix. figures 9 and 10 tests the ability of the algorithm to detect a bias of 10m and 20m on satellite number 3. Although that there is a hypothesis associated with the 10m bias on satellite 3, the algorithm was not able to converge on the correct hypothesis due to the existence of large noise magnitude on the satellite measurement. In the case of 20m bias level, there is no hypothesis for this bias magnitude. The algorithm did not converge on the closest hypothesis which is the 10m hypothesis due to large magnitude measurement noise level. The probability of the 10m hypothesis is shown in plot 3 of figures 9 and 10.

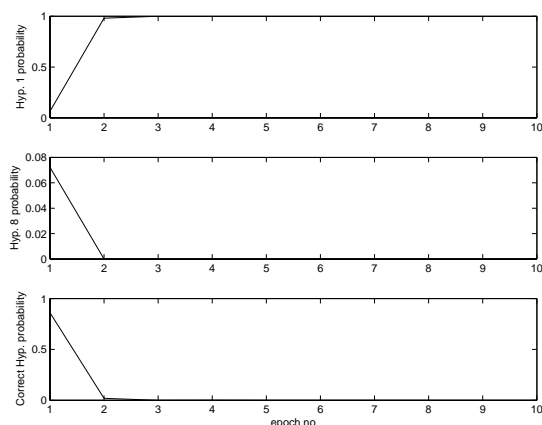


Fig. 9. Hyp. Probability, 10m-bias, Meas. Cov. = 12.5

### V. CONCLUSIONS

In this paper, a sequential integrity monitoring algorithm for detecting a bias error in the GPS pseudorange measurements

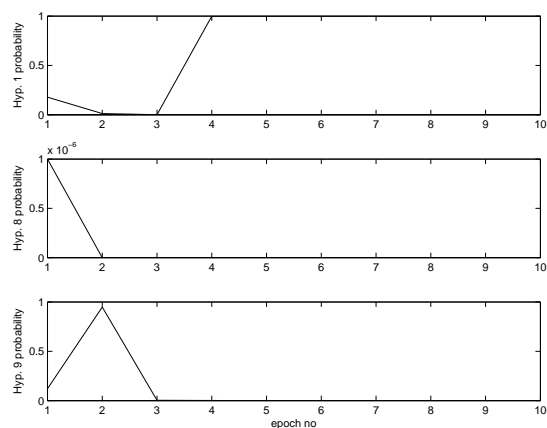


Fig. 10. Hyp. Probability, 20m-bias, Meas. Cov. = 12.5

is proposed. In the algorithm, a set of hypotheses are defined for possible bias levels in the satellites' measurements in view of the receiver. It was assumed that a bias error occur in one satellite at a time. Furthermore, the bias is detected before its magnitude could change. The probability for each hypothesis is then sequentially updated through the residual obtained from the received measurements and the estimate obtained from a GPS/IMU extended Kalman filter. The hypothesis with a probability that approaches one is declared the correct hypothesis. Simulation results were presented to show the accuracy of the proposed algorithm. It was seen that the algorithm successfully detects the correct bias level in the satellite measurements if their exists a hypothesis that is close to the existing GPS measurement bias. If the existing measurement bias is not among the hypothesis set, then the algorithm converges to the hypothesis close to the existing bias level. If the existing bias is in the middle of two hypotheses, then the algorithm, in time, divides the sure probability between the two hypotheses. The algorithm was seen not to converge properly on the correct hypothesis if the measurement noise covariance is big in comparison to the true bias in the GPS measurement. The presented algorithm is crucial for GPS measurements integrity monitoring.

### REFERENCES

- [1] P. S. Maybeck, *Stochastic Models, Estimation and Control, Volume 1*, Navtech Book and Software Store, Arlington, VA, 1994.
- [2] B. Hofmann-Wellenhof, H. Lichtenegger, and J. Collins, *GPS Theory and Practice*, 4th Ed., Springer-Verlag/Wien, New York, 1997.
- [3] B. W. Parkinson and J. J. Spiker, *Global Positioning System: Theory and Applications*, Vol. 1 and 2, American Institute of Aeronautics and Astronautics, Inc., Washington D.C., 1996.
- [4] J. A. Farrel and M. Barth, *The Global Positioning System and Inertial Navigation*, McGraw Hill, San Francisco, 1999.
- [5] B. J. Odelson, M. R. Rajamani, and J. B. Rawlings, *A new Autocovariance Least-Squares Method for Estimating Noise Covariances*, *Automatica*, no. 42, no. 3, pp. 303-308, 2005.
- [6] B. J. Odelson, A. Lutz, and J. B. Rawlings, *The Autocovariance Least-Squares Method for Estimating Covariances: Applications to Model-Based Control of Chemical Reactors*, *IEEE Transactions on Control Systems Technology*, Vol. 14, No. 3, pp. 532-540, 2006.
- [7] N. A. White, P. S. Maybeck, and S. L. DeVilbiss, *Detection of Interference/Jamming and Spoofing in a DGPS-Aided Inertial System*, *IEEE Transactions on Aerospace and Electronic Systems*, Vol. 34, No. 4, pp. 1208-1217, 1998.

- [8] M. Wei and K. P. Schwarz, *A strapdown inertial algorithm using an Earth-fixed Cartesian frame*, Navigation, Journal of the Institute of Navigation, Vol. 37, No. 2, pp. 153-167, 1990.
- [9] S. Hong, M. Lee, J. Rios, and J. L. Speyer, *Observability Analysis of GPS Aided INS*, Proceedings of the 2000 Institute of Navigation, Salt Lake City, UT, Sept. 2000.
- [10] W.R. Williamson, M.F. Abdel-Hafez, I. Ree, E. Song, J. Wolfe, D. Cooper, and J. L. Speyer, *An Instrumentation System Applied to Formation Flight*, IEEE Transactions on Control Systems Technology, vol. 15, No. 1, pp. 75-85, 2007.
- [11] I. Rhee, M.F. Abdel-Hafez, and J.L. Speyer, *On the Observability of Strapdown INS System During Maneuvers*, IEEE Transactions on Aerospace and Electronic Systems, Vol. 40, No. 2, pp. 526-536, 2004.

**Mamoun F. Abdel-Hafez** is an Assistant Professor in the Department of Mechanical Engineering at the American University of Sharjah. He received his B.S. in Mechanical Engineering from Jordan University of Science and Technology in 1997, his M.S. in Mechanical Engineering from the University of Wisconsin, Milwaukee in 1999, and his Ph.D. degree in Mechanical Engineering from the University of California, Los Angeles (UCLA) in 2003. Dr. Abdel-Hafez served as a Post Doctoral Research Associate in the Department of Mechanical and Aerospace Engineering at UCLA from June, 2003 to December, 2003, where he was involved in a research project on fault-tolerant autonomous multiple aircraft landing. His research interests are in stochastic estimation, control systems, and algorithms and applications of GPS/INS systems.